Journal of Network Intelligence
Taiwan Ubiquitous Information
 ISSN 2414-8105
Volume **9**, Number **4**, November **2024**

Vibration Signal Feature Extraction of Wu's Shallow Acupuncture Based on CV-SVM

Weidong Fang

School of Electronic, Electrical Engineering and Physics
Fujian Provincial Key Laboratory of Automotive Electronics and Electric Drive
Fujian University of Technology, Fuzhou 350118, China
wdfang@126.com

Zebin Chen*

School of Electronic, Electrical Engineering and Physics
Fujian Provincial Key Laboratory of Automotive Electronics and Electric Drive
Fujian University of Technology, Fuzhou 350118, China
2201905107@smail.fjut.edu.cn

Jeng-Shyang Pan

College of Computer Science and Engineering
Shandong University of Science and Technology, Qingdao 266590, China
Chaoyang University of Technology, Taichung 413310, Taiwan
jengshyangpan@gmail.com

*Corresponding author: Zebin Chen

Received May 4, 2023, revised September 11, 2023, accepted April 22, 2024.

Abstract. *Wu Binghuang shallow acupuncture technique was selected as the sixth batch of intangible heritage items in Fujian Province in 2019, and Wu Binghuang shallow acupuncture technique has good effect on treating insomnia in clinical trials. The shallow acupuncture technique has three kinds of techniques: " drainage method", " tonic method", and " flat tonic and flat drainage", which can be used for different treatment purposes, and the three techniques have high operational similarity. In the development of the shallow needle instrument using modern electronic technology to simulate the shallow needle technique of Bing-Huang Wu, it is necessary to extract and distinguish the vibration signals of the three modes. To address the problem of difficulty in differentiating Wu's shallow acupuncture techniques, a feature extraction method based on EMD sample entropy, energy occupation ratio after Pyramid decomposition and CV-SVM is proposed in this paper. The vibration signal is noise reduced by using wavelet noise reduction, firstly, the EMD decomposition is performed on the noise reduced data, the correlation coefficient between individual IMF and the original signal is calculated, the IMF with the correlation coefficient greater than 0.1 is selected as the effective component, the sample entropy of the effective component is calculated, then the Pyramid decomposition of the noise reduced vibration signal is divided into 9 layers, the relative energy of each layer is calculated, and the sample entropy of the effective component and the relative energy of each layer are calculated. The sample entropy of the effective component and the relative energy of each layer are formed into a Govett collection. The CV-SVM is then employed to identify the signal patterns, resulting in an average recognition rate of 76% that possesses engineering application value. The vibration data of Prof. Wu Binghuang's treatment with shallow needles were analyzed, and the practical application of the proposed method in distinguishing the vibration signals of the three techniques of Wu Binghuang's shallow needling was verified. The implementation results show the outstanding practicality and scalability of our proposed scheme.*

Keywords: Vibration Signal, Wavelet Noise Reduction, Sample Entropy, Frequency distributio, CV-SVM

1. **Introduction.** Wu Binghuang shallow acupuncture [1] mainly uses modulator needles, using the middle finger nail on the needle handle to make a continuous scraping and pushing action to make the needle handle vibrate rapidly and continuously, which is conducted through the body and tip of the needle to the meridian point where it produces a gentle stimulation to guide the needle sensation of soreness, swelling, and numbness [2]. It can be seen that manually scraping the needle body to make it vibrate is the main method of stimulating acupuncture points. The " scratching and crawling" technique from the lower end of the needle shank to the top of the needle shank is called the " scraping" method and the opposite is called the " pushing" method. Treatment techniques three techniques are drainage method, tonic method and flat tonic flat drainage method. The operation of the laxative method needle body is not perpendicular to the skin where the empty space for the upper scraping heavy, light pushing down. Tonic method of operation when the needle body is perpendicular to the skin plane where the acupuncture point is located when the technique is light when scraping, pushing down the technique is heavy. In the flat tonic and flat diarrhea operation, the needle body alternates between vertical and non-vertical continuous oscillation with the skin plane where the acupuncture point is located, with light upward scraping and light downward pushing [3]. Different manipulations with different force and speed produce different vibration frequencies. During the treatment, the doctor will choose different treatment techniques according to the different conditions of different patients [4]. Thus, it can be seen that the correct use of different techniques of shallow needles by medical students is one of the key factors in the correct treatment of diseases, and shallow needles are difficult to operate, medical students need to spend a lot of time figuring out and training, and whether the correct mastery of the

three techniques need to be evidenced according to the treatment situation, this situation will reduce the effectiveness of treatment, and the learning efficiency of medical students is low.

The Modern scholars are using modern information technology, artificial intelligence and electronics to solve traditional problems [5, 6, 7, 8]. The vibration signal is widely used as a signal characteristic quantity in several fields, Shi applied it in the agricultural industry as a fault diagnosis signal on combine harvesters [9], Liu et al. applied it in the electric power industry as a method for identifying the state of the operating mechanism of circuit breakers [10], Xuan et al. applied it in the metalworking industry as a diagnosis of rail defects [11], and Wang et al. applied it to the motor on as a judgment signal of motor speed [12]. With the development of the industry, vibration signals are used more and more frequently, but there is inevitably noise in the process of collecting vibration signals, so the collected signals need to be processed for noise reduction as a way to reduce errors. Wavelet threshold denoising is the method with less computation and better filtering effect among noise reduction methods, but the selection of wavelet bases and different threshold rules will produce different noise reduction effects, and we need to choose the combination of wavelet bases and threshold rules with optimal effects [13].

SMO and SVM classification algorithms are more widely used with the rapid development of cloud computing [14, 15, 16]. CV-SVM (Cross-Validation Support Vector Machines) is a model selection method based on the SVM algorithm, which determines model parameters by cross-validation to improve the generalization ability of the model [17, 18, 19]. In CV-SVM, the data set is divided into K equal-sized subsets, one of which is used as the validation set and the remaining K*-1* subsets are used as the training set. This process is repeated K times, each time using a different subset as the validation set and the remaining subsets as the training set. Eventually, the average performance of the model can be calculated and used to select the optimal model parameters [20].

Sample entropy is a statistical method based on information theory that measures the uncertainty or randomness of the data. It is calculated based on the frequency distribution of individual values in a sample. Sample entropy can be used to measure the complexity or irregularity of a signal, or it can be used for feature selection in classification or clustering analysis [21]. In sample entropy, the data are treated as discrete random variables, which can take values that are either continuous or discrete. To calculate the sample entropy, the data needs to be divided into several intervals, then the frequency distribution of each value taken in each interval is calculated, and finally the sample entropy is calculated according to the definition of information entropy. The higher the sample entropy, the greater the randomness and uncertainty of the data [22].

EMD (Empirical Mode Decomposition) is a local signal decomposition method that decomposes complex nonlinear and non-stationary signals into a set of " Intrinsic Mode Functions" (IMFs). The basic signals. Each IMF represents a frequency component of the signal, and they satisfy the definition of intrinsic mode functions, i.e., the average value of the upper and lower envelopes of each IMF is zero over the entire time and frequency range, and the frequencies and amplitudes of IMFs do not overlap with each other. EMD can be applied to many fields, examples include signal processing, image processing [23], feature extraction [24], etc.

In this paper, we propose a method of differential characterization based on vibration signals, and collect vibration data from Professor Bing-Huang Wu, who has mastered the three techniques. After obtaining the noise-reduced data, the energy distribution of the original vibration data in different frequency bands can be obtained by decomposing the vibration signal into multiple frequency bands using the pyramid algorithm [25, 26] and normalizing the energy in each frequency band. And the 9-layer IMF is obtained by

EMD decomposition, and the sample entropy of each IMF is calculated. The combined features are input into CV-SVM for pattern recognition to achieve pattern differentiation and facilitate subsequent shallow needle instrument development.

2. **Experimental Data Acquisition.** The acquisition site is shown in Figure 1, the vibration data of the shallow needles used in this experiment were collected by the laboratory equipment with a sampling frequency of 1000 HZ, mainly including the data of three techniques of " Wu's shallow needle technique": tonic method, diarrhea method, and flat tonic and flat diarrhea method, and the main component of the data was the vibration data during the application of shallow needles. In this paper, the data of the three techniques were collected, including the flat tonic and flat diarrhea method, the tonic method and the cathartic method. The data for each manipulation were 40 groups each, and each group was 4096 data. The differences in vibration signals of the three techniques were mainly generated by the different strengths.

FIGURE 1. On-site photo collection

(1) Average patch and vent therapy: As shown in Figure 2, during this maneuver the upward scraping and downward pushing keep the force even, so that the needle body keeps even vibration. The average patch and vent therapy data collected during the operation of Professor Bing-Huang Wu are shown in Figure 3.

(2) Patch therapy: As shown in Figure 4, this maneuver is operated with light upper scraping and heavy lower pushing, which makes the needle body show uneven vibration, and the Patch therapy data collected during the operation of Professor Bing-Huang Wu is shown in Figure 5.

(3) Vent therapy: As shown in Figure 6, this technique is operated with heavy upper scraping and light lower pushing, which makes the needle body present a different uneven vibration from the tonic method, and the patch therapy data collected during the operation of Professor Bing-Huang Wu is shown in Figure 7.

3. **The Current State Of Development Of Research Methods.** Traditional signal analysis methods cannot overcome the effects caused by signal noise and time variability. And wavelet analysis can better solve this problem [27]. Wavelet analysis is a new branch of mathematics and is the result of research in several mathematical fields. It is considered as another effective way of frequency analysis in application fields, especially in image integration [28], fault diagnosis [29, 30], face recognition [31] and many nonlinear sciences. Wavelet transform has better time and frequency domain characteristics

FIGURE 2. Schematic diagram of the single-round operation of flat patch and flat drain

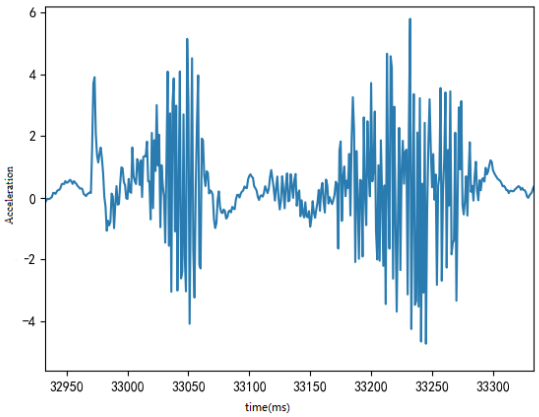

FIGURE 3. Average patch and ventilation therapy

compared to Fourier transform, which can efficiently extract and analyze signals and can well improve the limitations of Fourier transform in time variability. The advantages of wavelet transform over Fourier transform determine [32] that it will be widely used in various fields of research and engineering, especially in fault diagnosis [31, 33], image fusion [28, 34], algorithm research [35, 36, 37, 38], feature extraction [39, 40] and many other fields.

FIGURE 4. Diagram of the single-round operation of the mending method

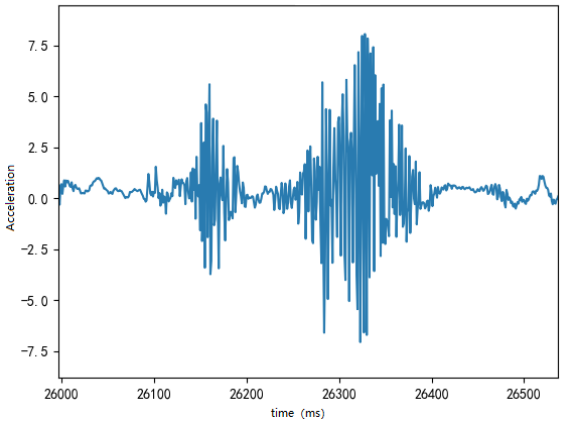

FIGURE 5. Patch therapy

3.1. **Pyramid Algorithm.** After obtaining the noise-reduced signal data, this paper will carry out signal feature extraction. In the study of vibration signals with high recognition, the frequency distribution of the signal can be decomposed by the pyramid algorithm, and then the energy of each frequency band is calculated and normalized, and then the

FIGURE 6. Diagram of the single-round operation of the drainage method

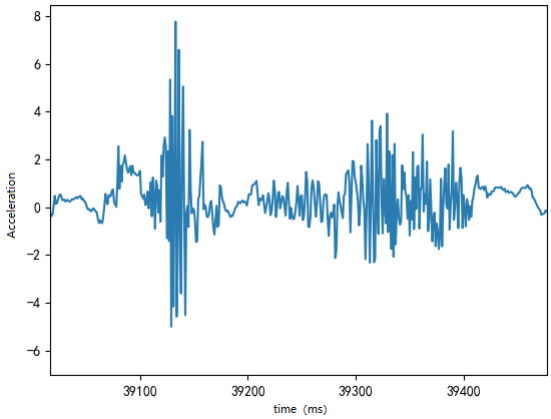

FIGURE 7. Vent therapy

difference features are derived by comparing the energy distribution, which has been applied to the medical field in the literature [41]. The basic principle of the pyramid algorithm is to decompose the signal in multiple levels of wavelets, i.e., the approximate sequence aj of the decomposition result of the previous level is decomposed again, which can get the approximate sequence $aj1$ and the detail sequence $dj1$, and so on. Until any specified number of levels of multilevel wavelet decomposition, as shown in Figure 8. Finally all detail sequences $dj, \ldots, d1$ the lowest level approximation sequence aj need to be retained, and other approximation sequences need not be retained.

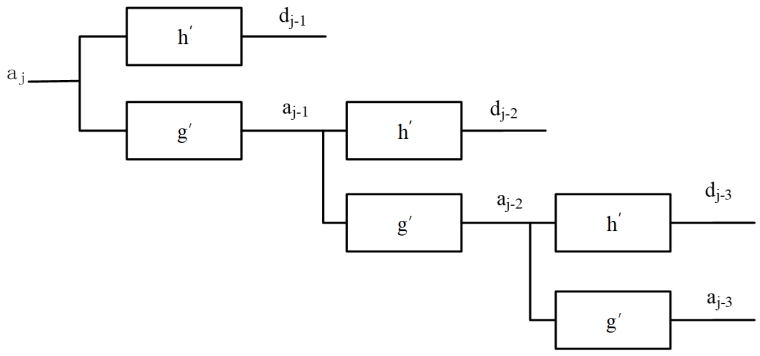

FIGURE 8. Frequency diagram

This paper uses the pyramid algorithm to analyze the frequency components from the sampled input signal, which can obtain the energy distribution in different frequency bands, and after normalization, the energy share of each frequency band can be obviously derived, based on the energy distribution to explore the difference characteristics between different techniques.

3.2. **Wavelet Decomposition and Reconstruction.** The wavelet transform itself has the property of multi-resolution analysis, which allows wavelet analysis to have a more refined analysis of the signal. The wavelet transform is defined as Formula (1).

$$W_f(a,b) = \int_{-\infty}^{+\infty} f(t)\psi_{a,b}(t)dt = \int_{-\infty}^{+\infty} f(t)a^{\frac{1}{2}}\psi(\tfrac{t-b}{a})dt \tag{1}$$

Its inverse conversion is Formula (2).

$$f(t) = \tfrac{1}{C_\psi}\int_{-\infty}^{+\infty}\int_{-\infty}^{+\infty} a^{-2}w_f(a,b)\psi_{a,b}(t)dadb \tag{2}$$

in the Formula (3)

$$C_\psi = \int_{-\infty}^{+\infty} \tfrac{|\psi(\omega)|^2}{\omega}d\omega < \infty \tag{3}$$

Where ψ is the Fourier transform. Wavelet transform can be divided into continuous wavelet transform as well as discrete wavelet transform according to the continuity and dispersion of the processed signal, and according to the dimensionality of the signal, it can be divided into one-dimensional transform and two-dimensional transform. Since the data used in this topic is one-dimensional discrete data, the one-dimensional discrete wavelet transform used is introduced, which is as follows. Let $\psi(t) \in L^2(R)$, then its Fourier transform can be expressed as $\widehat{\psi}(\overline{\omega})$, and the complete reconstruction condition of the signal $\widehat{\psi}(\omega)$ is as follows Formula (4)

$$C_\psi = \int_R \frac{|\widehat{\psi}(\omega)|^2}{|\omega|} d\omega < \infty \tag{4}$$

When the above conditions are met, we call $\psi(t)$ the mother wavelet. Using the telescopic translation property of wavelet transform itself to transform $\psi(t)$, we can obtain Formula (5)

$$\psi_{a,b}(t) = \frac{1}{\sqrt{|a|}} \psi(\frac{t-b}{a}) \tag{5}$$

where $a, b \in R, a \neq 0$ are the scaling and translational factors of the signal, respectively. So for any function K, when it satisfies the above condition, i.e., $A = B$, we can describe its wavelet decomposition as Formula (6)

$$W_f(a,b) =< f, \psi_{a,b} >= |a|^{-\frac{1}{2}} \int_R f(t) \overline{\psi(\frac{t-b}{a})} dt \tag{6}$$

The inverse conversion is Formula (7)

$$f(t) = \frac{1}{C_\psi} \int_{-\infty}^{+\infty} \int_{-\infty}^{+\infty} \frac{1}{a^2} W_f(a,b) \psi(\frac{t-b}{a}) da db \tag{7}$$

Because the wavelet $\psi(t)$ generated by the transformation of the mother wavelet $\psi_{a,b}(t)$ is similar to a " window function" in the analysis of the signal, $\psi(t)$ must also satisfy the convergence conditions required for a general wavelet function.

$$\int_{-\infty}^{+\infty} |\psi(t)| dt < \infty \tag{8}$$

And in order for this signal to be reconstructed, the condition $\widehat{\psi}(\omega) = 0, \omega = 0$ must be satisfied and the Fourier transform of C must satisfy the stability condition.

$$A \leq \sum_{-\infty}^{\infty} |\hat{\psi}(2^{-j\omega})|^2 \leq B, 0 < A \leq B < \infty \tag{9}$$

3.3. **EMD decomposition.** The EMD algorithm description can be summarized as follows: for any signal, it consists of several finite eigenfunctions. And the essence of EMD is to decompose the signal into several eigenfunctions, and its decomposition process is as follows: Find the maximal and minimal values of the original data series $x(t)$, and synthesize all the maximal points into the upper envelope $e_{\max} t$ of the original data series by the third spline interpolation function, and similarly, synthesize all the minimal points into the original lower envelope $e_{\min} t$. The mean values of the upper and lower envelopes are used as the mean envelope $m(t)$ of the original data series:

$$m(t) = \frac{e_{\max}(t) + e_{\min}(t)}{2} \tag{10}$$

Find the difference $h_1^1(t)$ between $x(t)$ and $m(t)$: Generally speaking, $h_1^1(t)$ is an unstable signal, the definition of IMF requires that the total number of extreme points in the time domain must be equal to the total number of signal zeros, the number of differences between the two at most one, and in the time domain at any point in time, the average value of the upper and lower envelope must be 0. Unstable signal obviously does not meet this condition, so at this time $h_1^1(t)$ is not the IMF component of signal $x(t)$.

Repeat the operations described in Formula (11) and Formula (12), assuming that until the kth time, the resulting $h_1^k(t)$ satisfies the conditions defined by the IMF, at which point we can consider $h_1^k(t)$ to be the first-order IMF component $c_1(t)$ of the original data series $x(t)$.

$$c_1(t) = imf_1(t) = h_1^k(t) \tag{11}$$

The above operation is repeated to obtain the second-order IMF component $c_2(t)$ of the original data sequence $x(t)$ and the remaining IMF components, until the decomposition process ends when the remaining part of the original data sequence $x(t)$ is a monotonic sequence or the residual $r_n(t)$ of a constant sequence. The result of the decomposition can be expressed as

$$x(t) = \sum_{i=0}^{n} c_i(t) + r_n(t) \tag{12}$$

4. **Wavelet transform-based noise reduction of vibration signals.** Wavelet transform is a method for analyzing local variations of signals, and its idea is derived from the unfolding and displacement method. It is both an inheritance and development of the concept of short-time Fourier transform and an overcoming of the fact that short-time Fourier transform cannot provide ideal spatial and frequency resolution at the same time.

4.1. **Wavelet denoising principle.** In practical engineering applications, the signals we detect are often mixed with different noises. In a broad sense, except for our useful components, all the remaining parts within the signal are useless signals, i.e., noise. So, we can define a signal in the following form Formula (13).

$$h(t) = f(t) + x(t) \tag{13}$$

where $h(t)$ is our detected signal, while $f(t)$ is the useful component and $x(t)$ is the noise. Within wavelet analysis, there are three types of threshold selection methods for threshold noise reduction, which are threshold denoising, wavelet-based correlation denoising and wavelet analysis based on the principle of great value denoising. Among them, threshold denoising is a denoising method with better denoising effect and simpler implementation process. The basic idea of denoising is: firstly, wavelet decomposition is performed on the pre-denoised signal, a threshold is set, the part of the wavelet coefficients in each layer of the decomposition that is larger than the wavelet coefficients in this layer is denoised, and then the reverse reconstruction is performed to obtain the denoised signal of the original signal. By further specifying equation Formula (13), it can be written as Formula (14).

$$h(t) = f(t) + \sigma x(t) \tag{14}$$

Where σ is the intensity of the noise within the signal. The purpose of wavelet transform is to suppress or eliminate the noise $x(t)$ within the signal $h(t)$ by decomposition calculation in order to get a more intact and useful signal $f(t)$. After determining the thresholding rules, the signal can be selected as hard or soft thresholding to perform noise reduction. Hard thresholding is to keep the part of the decomposition coefficients greater than the threshold α and replace the part less than the threshold α with 0. This method will cause the signal to produce intermittent effect at the discontinuity with large difference. Soft thresholding avoids the discontinuity by strengthening the contraction at the discontinuity. Hard threshold method, when the absolute value of the wavelet coefficients is greater than the set threshold, it will remain unchanged, and if it is less than the set threshold then make it 0, which is defined as the Formula (15).

$$W_\lambda = \begin{cases} w, |w| \geq \lambda \\ 0, |w| < \lambda \end{cases} \tag{15}$$

The soft threshold method is defined in Formula (16), if the absolute value of the wavelet coefficients is greater than the set threshold value, make it subtract the threshold

value. If it is less than the set threshold, it is set to zero as the hard threshold.

$$W_\lambda = \begin{cases} [\text{sgn}(w)(|w| - \lambda)], |w| \geq \lambda \\ 0, |w| < \lambda \end{cases} \tag{16}$$

4.2. **Wavelet Noise Reduction.** Needle body in the process of use, and not continuous vibration, in between each cycle there is a small period of no vibration signal exists in the interval, but from the actual data collected, there is a weak signal in this section of the interval, the vast majority of this signal is the noise signal, which is the most obvious part of the signal data noise signal. By observation, it can be seen that the noise signal is relatively smooth and low energy. So in the original signal doped with noise signal, the noise energy is much lower than the vibration signal, which is less disturbing for the further study conducted in this paper. However, in order to improve the accuracy, this paper uses wavelet noise reduction for noise reduction processing. We hope to achieve both to retain the effective end of the vibration signal and to reduce the noise energy of the invalid part as much as possible.

(1) Commonly used wavelet basis functions are haar wavelet, dbN wavelet, symlet wavelet, coif wavelet, fk wavelet, etc. The properties of commonly used wavelets are summarized in Table 1, which include orthogonality, biorthogonality, Compact support, DWT, CWT, Support width, Filters length, Symmetry.

(2) Support length. The support interval of the wavelet function is the length that can converge from a finite value to 0. In general, the wavelet transform has a strong discriminative power for high-frequency components, but is weak for low-frequency components. The size of the support length is directly related to the time to calculate the wavelet decomposition, so it should not be too large in the practical application process.

(3) Symmetry. Wavelet function generated by the filter and the traditional sense of the window function and other filters, such as different, it has phase linearity, that is, symmetry, the better the symmetry of the wavelet function, the better the filtering effect.

(4) Vanishing moment. It is defined as:

$$\int t^p \psi(t) dt = 0 \tag{17}$$

where ψ(t) is the fundamental wave. When satisfied $0 \leq p < N$, the wavelet function is said to have an Nth order vanishing moment. Regularity

(5) Similarity. In practical applications, wavelets similar to the signal waveform should be selected

Table 1. Common wavelet function

Common wavelet functions	Haar	symN	dbN	Coif N
Orthogonality	yes	yes	yes	yes
Biorthogonality	yes	yes	yes	yes
Compact support	yes	yes	yes	yes
DWT	possible	possible	possible	possible
CWT	possible	possible	possible	possible
Support width	1	2N-1	2N-1	6N-1
Filters length	2	2N	2N	6N
Symmetry	yes	Near from	far from	Near from
Number of vanishing moments for psi	1	N	N	2N

The symlets wavelet is a wavelet transform based on multi-resolution analysis and multi-sampling filter theory, which is applicable to wavelet transform of discrete sequences, usually expressed as sym N. The waveform of coif wavelet is approximately symmetric, and it does not have specific expressions and wavelet bases. The vibration signals collected in this paper are discrete signals and have characteristics such as nonlinearity and non-smoothness. For the research carried out in this paper, wavelet basis functions with orthogonality and symmetry are required, while wavelet basis functions with tight support can reduce computational effort and avoid signal distortion. Symlets wavelets established on the basis of multi-sampling rate filters and multi-resolution analysis theory have better orthogonality, symmetry and tight support, and can perform noise reduction on acceleration signals in soft threshold mode, and for acceleration signal processing experiments prove that symlets wavelet family basis functions have good noise reduction effect on vibration signals, and we finally choose symlets wavelet family as the basis function in soft thresholding mode and choose the thresholding rule with it by experiment.

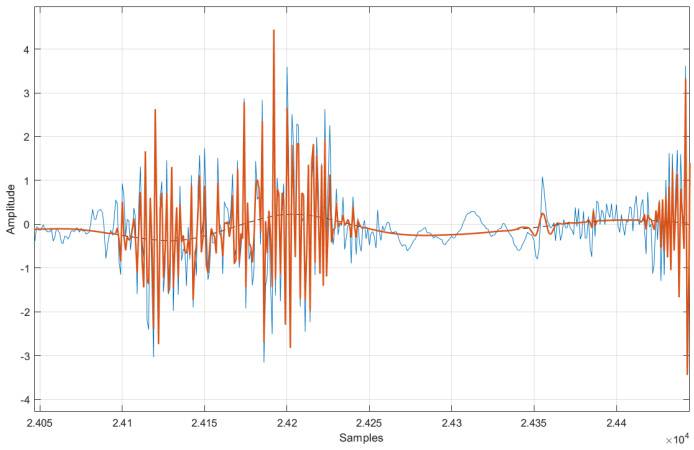

FIGURE 9. Empirical Bayes Threshold Rule

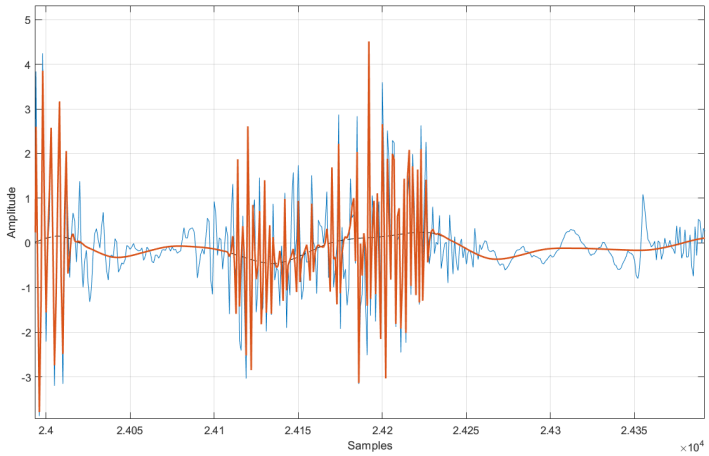

FIGURE 10. False Discovery Rate Threshold Rule

The threshold rules paired with Figure 9 and Figure 10 are Empirical Bayes and False Discovery Rate, and the threshold rule paired with Figure 11 is Stein's Unbiased Risk Estimate. From the comparison of the time domain plots before and after the original

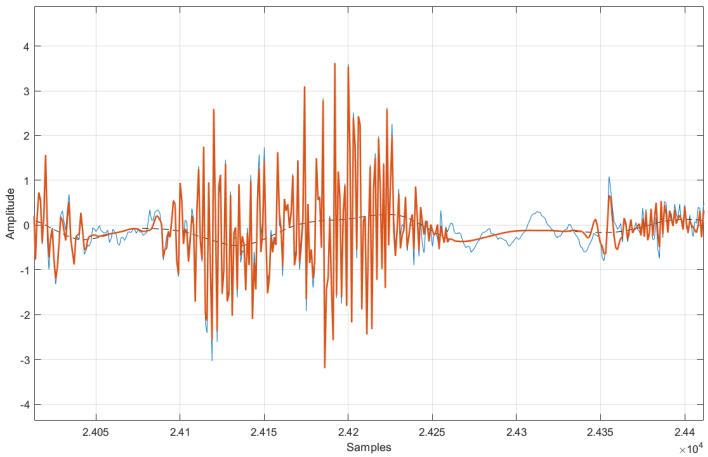

FIGURE 11. Stein's Unbiased Risk Estimate Threshold Rule

signal denoising, it can be seen that Figure 9 and Figure 10 can reduce the interference signal of the invalid fragment, but for the effective The signal of the effective fragment is too much reduced. After the threshold noise reduction with Stein's Unbiased Risk Estimate, the effective signal is fully retained and the rest of the noise is filtered out, which is good and meets the noise reduction purpose.

5. **Wu's shallow needle technique feature extraction.**

5.1. **Wavelet pyramid based algorithm for vibration signal feature extraction.**

Because of the high similarity of the three techniques, it is crucial that the same operator operates the three techniques so that their energies show a regular distribution, but it is inevitable that the three techniques also have a high similarity. Therefore, we investigate the relative deviation of the frequency energy distribution to distinguish and evaluate the accuracy of the operators. As shown in Figure 12, the energy signal of the lower interference signal has been obtained, and the signal is decomposed into 9 layers by pyramid decomposition.

The signal is decomposed into 9 layers, and the wavelet coefficients of each layer are obtained. The larger the square of the coefficients, the greater the energy of that frequency band, and the energy of different layers can be calculated according to Formula (18).

$$E\_d_{(k)} = \sum_{i=1} \left| C\_d_{(k)}(i) \right|^2 \tag{18}$$

The total energy of the signal E_t is the sum of the energy of each layer.

$$E\_t = \sum_{k=1}^{9} E\_d_{(k)} \tag{19}$$

The energy $E_d(k)$ of the different layers divided by the total energy E_t is equal to the ratio of the energy of the signal in the different frequency bands.

$$P\left[E\_d_{(k)}\right] = \left[\frac{E\_d_{(k)}}{E\_t}\right] \tag{20}$$

AS shown in Figure 13,the vibration signals of the three maneuvers were divided and the energy distribution of the different maneuvers was obtained after calculation by Formula (18), Formula (19) and Formula (20). Calculate the energy distribution of each layer after the pyramidal decomposition of the vibration signals of different maneuvers, and get Table 2.

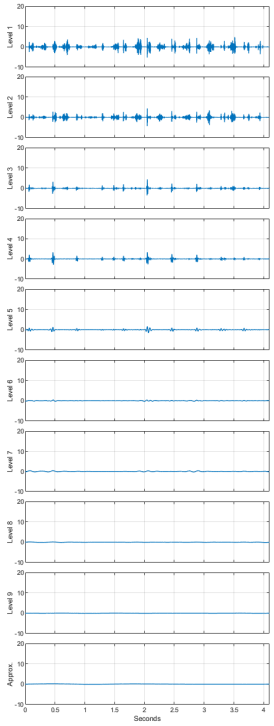

FIGURE 12. Level 1 to 9 diagram

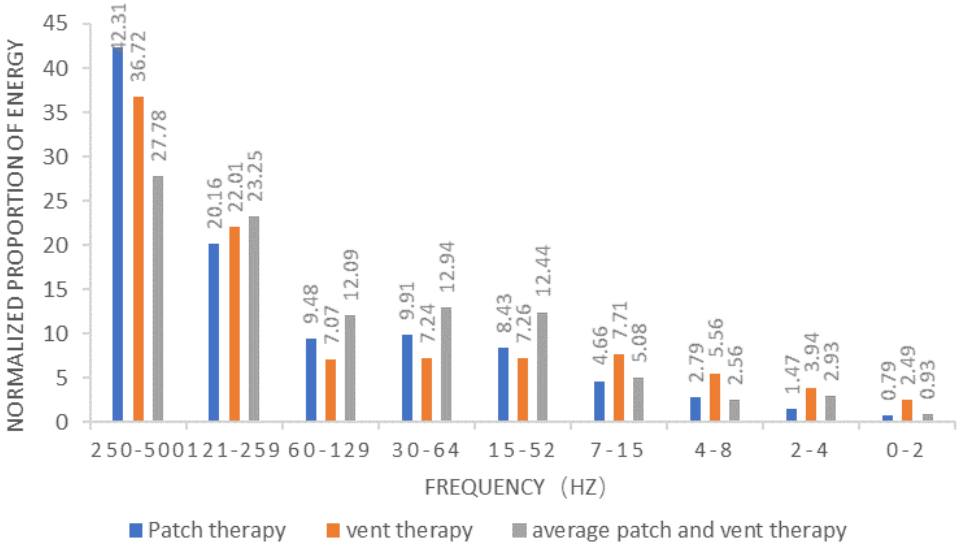

FIGURE 13. Energy distribution map

5.2. **EMD-based sample entropy feature extraction for vibration signals.** The EMD decomposition of the vibration signal after noise reduction, the decomposition of the three maneuvers is shown in Figure 14. The correlation coefficients of individual IMF components and the original signal are calculated, and the correlation coefficient screening threshold is set to 0.1, and the calculation results are shown in Figure 15. It can be seen from Figure 15 that the effective modal components of the tonic method are IMF1-IMF3,

TABLE 2. Frequenc energy distribution of each layer after decomposition of Pyramid by different techniques

	Sample number	Energy share per layer(%)								
		level1	level2	level3	level4	level5	level6	level7	level8	le
Patch therapy	3	49.37	24.58	11.09	9.51	4.05	0.57	0.11	0.05	0
	4	62.78	20.16	7.50	5.75	2.99	0.49	0.15	0.02	0
	5	59.50	19.69	9.09	6.35	4.10	0.69	0.09	0.01	0
Average therapy	50	38.23	31.09	10.41	10.29	7.38	1.64	0.63	0.10	0
	51	38.36	27.02	12.95	12.99	6.92	1.16	0.33	0.05	0
	52	35.19	29.97	13.21	12.09	7.67	1.27	0.37	0.05	0
Vent therapy	81	41.07	27.08	10.78	8.11	8.27	2.95	0.83	0.15	0
	82	42.66	22.48	9.85	9.08	8.53	3.88	1.69	0.18	0
	83	53.52	24.71	7.12	6.23	5.06	1.47	0.77	0.13	0

the effective modal components of the flat tonic and flat diarrhea method are IMF1-IMF3, and the effective modal components of the drain method are IMF1-IMF3, so the feature set for constructing the input classifier is the sample entropy of IMF1-IMF3, and the sample entropy feature values of different techniques are calculated as in Table 3.

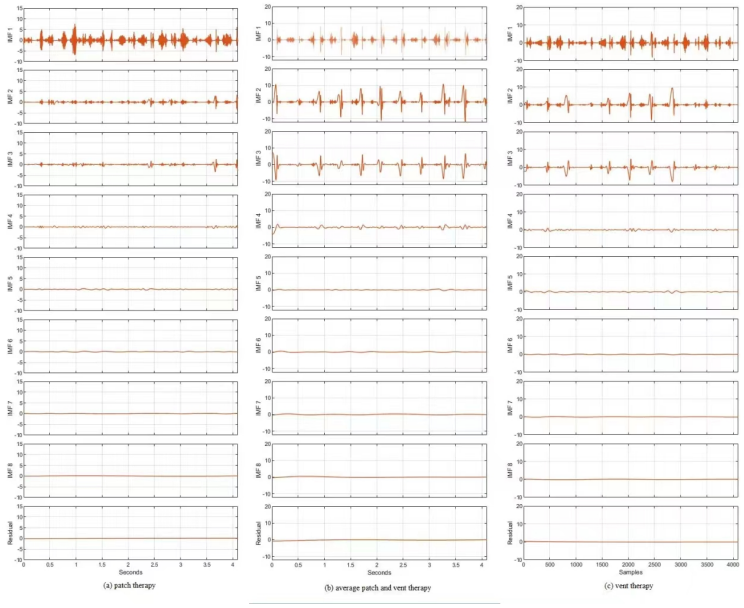

FIGURE 14. Vibration signal EMD decomposition results

The sample entropy of the effective components of the three maneuvers was calculated to obtain Table 3.

60 sets of samples are randomly selected as the training set, i.e., 20 sets of each maneuver are randomly selected, and the remaining samples are used as the test set. CV-SVM was used for pattern recognition of the samples, and after the samples were input into CV-SVM, the classification results are shown in Figure 16. Labels 1, 2, and 3 represent the tonic method, the flat tonic and flat drain method, and the drain method, respectively.

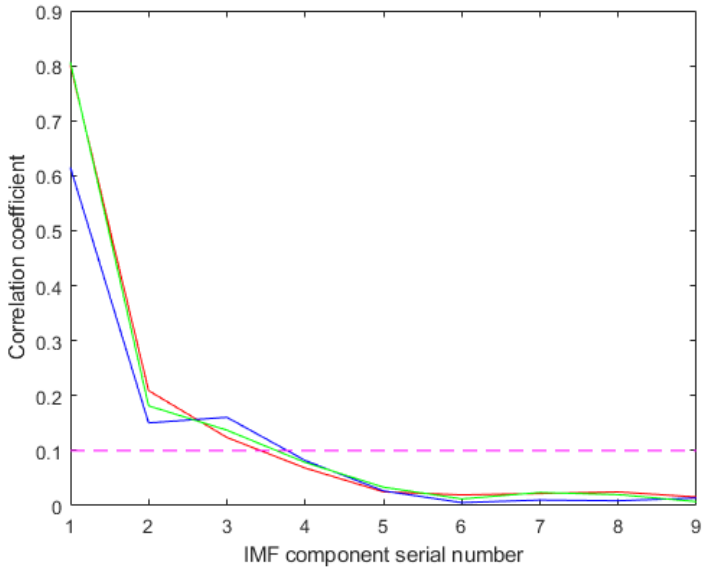

FIGURE 15. Correlation coefficients of IMF components of different mode signals

TABLE 3. Signal EMD sample entropy characteristics in different modes

Manipulation mode	Sample number	Sample entropy component		
		IMF1	IMF2	IMF3
Patch therapy	3	0.1665	0.1257	0.1067
	4	0.1760	0.1175	0.0889
	5	0.1715	0.1432	0.0814
Average patch and vent therapy	50	0.3847	0.2854	0.1634
	51	0.2898	0.1894	0.1426
	52	0.3306	0.2118	0.1298
Vent therapy	81	0.2559	0.2241	0.1545
	82	0.2561	0.1584	0.0996
	83	0.2412	0.1693	0.1056

As seen from the figure, the recognition rate reaches 78 % after the signal EMD sample entropy and the energy distribution after Pyramid decomposition are input into CV-SVM as feature values. To avoid the chance of the existence of one recognition, 30 trials were conducted with the same method, and the average recognition rate of the obtained results is 76

6. **Conclusion.** In order to investigate the differences in the mechanisms of the three techniques of " Wu's shallow needle technique", namely, the tonic method, the laxative method and the flat tonic and flat laxative method. The theoretical part of wavelet analysis applicable to this signal is studied, and the type of wavelet and the method of noise reduction are selected through experiments. Among the methods that can analyze the characteristics of vibration signals, the pyramid algorithm is selected as the main method for feature differentiation by comparing the methods in the relevant literature. In this paper, modern information acquisition techniques and analysis methods are used to

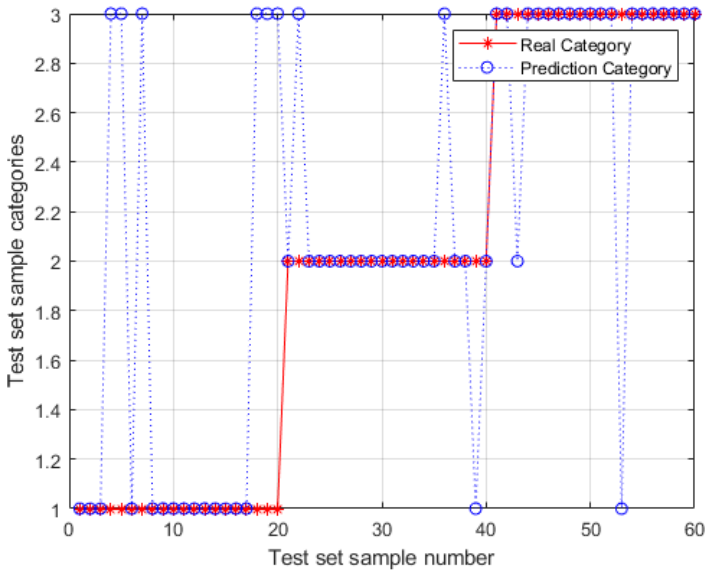

FIGURE 16. EMD sample entropy, pyramidal decomposition energy accounted for bits to solicit CV-SVM classification results

complete the research experiments. Based on MATLAB platform, the wavelet threshold noise reduction is applied, and then the pyramid algorithm is used to split the signal data into 9 frequency bands, extract the energy share of each band, and obtain the sample entropy of IMF components with correlation coefficient greater than 0.1 with the original signal through EMD decomposition, and construct the feature set by combining the energy share and sample entropy. The average recognition rate is 76% after inputting the energy share and sample entropy into CV-SVM, which has engineering application value. There are many aspects of this thesis that need further improvement and research. As a medical treatment evolved from ancient acupuncture, the shallow needle itself is worthy of our continuous research and development, but the shallow needle is not widely used in China at present, and the research of the shallow needle needs more domestic and foreign research scholars, medical personnel to participate.

Acknowledgment. This research was funded by Fujian Provincial Health Commission: 2020CXA053.

References

[1] Z. Wang, D. Gong, X. Yu, and S. Cai, "Wu binghuang's academic thought and clinical experience of regulating immune function by acupuncture and moxibustion," *Chinese Acupuncture & Moxibustion*, vol. 36, no. 8, pp. 861–863, 2016.

[2] X. Zheng, D. Gong, and P. Li, "Examples of clinical experience of prof. wu binghuang using acupuncture and moxibustion," *Modern Journal of Integrated Traditional Chinese and Western Medicine*, no. 06, pp. 724–725, 2005.

[3] X.-Z. Zhang and L.-D. Chen, "Clinical application of superficial acupuncture therapy on insomnia," *Smart Healthcare*, vol. 1, no. 03, pp. 58–62, 2015.

[4] D. Gong and Z. Wang, "Summary of professor wu binghuang's experience in treating insomnia in six ways," *Rehabilitation Medicine*, no. 04, pp. 50–51, 2008.

[5] T.-Y. Wu, A. Shao, and J.-S. Pan, "Ctoa: Toward a chaotic-based tumbleweed optimization algorithm," *MATHEMATICS*, vol. 11, no. 10, MAY 17 2023.

[6] L. Wang, Y. Lin, T. Yao, H. Xiong, and K. Liang, "Fabric: Fast and secure unbounded cross-system encrypted data sharing in cloud computing," *IEEE Transactions on Dependable and Secure Computing*, vol. 20, no. 6, pp. 5130–5142, 2023.

[7] T.-Y. Wu, H. Li, and S.-C. Chu, "Cppe: An improved phasmatodea population evolution algorithm with chaotic maps," *MATHEMATICS*, vol. 11, no. 9, APR 22 2023.
[8] C.-M. Chen, S. Lv, J. Ning, and J. M.-T. Wu, "A genetic algorithm for the waitable time-varying multi-depot green vehicle routing problem," *SYMMETRY-BASEL*, vol. 15, no. 1, JAN 2023.
[9] Y. Shi, "Research on the fault detection system of combine harvester based on vibration signal analysis," *Journal of Agricultural Mechanization Research*, vol. 45, no. 05, pp. 249–253, 2023.
[10] H. Liu, W. Xu, S. Zhao, E. Wang, and J. Liu, "State identification method of circuit breaker operating mechanism based on time course waveform and adaptive spectrum fusion analysis of vibration signal," *High Voltage Engineering*, pp. 1–10, 2022, j/OL. [Online]. Available: https://doi.org/10.13336/j.1003-6520.hve.20220795
[11] C.-F. Xuan, Y. Zhou, and Y. Liang, "Surface defect identification of rolling linear guideway based on vibration signal," *Modular Machine Tool & Automatic Manufacturing Technique*, vol. 2022, no. 07, pp. 144 147+151, 2022.
[12] W. Wang, H. Luo, T. Peng, and K. Xu, "A method of calculating motor speed based on vibration signal," *Explosion-Proof Electric Machine*, vol. 57, no. 02, pp. 27–30+42, 2022.
[13] J. Zhong, S. Jian, C. You, and X. Yin, "Wavelet de-noising method with threshold selection rules based on snr evaluations," *Journal of Tsinghua University (Science and Technology)*, vol. 54, no. 2, pp. 259–263, 2014.
[14] H. Xiong, Z. Qu, X. Huang, and K.-H. Yeh, "Revocable and unbounded attribute-based encryption scheme with adaptive security for integrating digital twins in internet of things," *IEEE Journal on Selected Areas in Communications*, vol. 41, no. 10, pp. 3306–3317, 2023.
[15] A. L. H. P. Shaik, M. K. Manoharan, A. K. Pani, R. R. Avala, and C.-M. Chen, "Gaussian mutation-spider monkey optimization (gm-smo) model for remote sensing scene classification," *REMOTE SENSING*, vol. 14, no. 24, DEC 2022.
[16] H. Xiong, H. Wang, W. Meng, and K.-H. Yeh, "Attribute-based data sharing scheme with flexible search functionality for cloud-assisted autonomous transportation system," *IEEE Transactions on Industrial Informatics*, vol. 19, no. 11, pp. 10 977–10 986, 2023.
[17] I. S. Mangkunegara and P. Purwono, "Analysis of dna sequence classification using svm model with hyperparameter tuning grid search cv," in *2022 IEEE International Conference on Cybernetics and Computational Intelligence (CyberneticsCom)*. IEEE, 2022, pp. 427–432.
[18] W. Wang, K. He, Y. Jin, F. Mo, X. Zhao, J. Pi, and X. Zhihuai, "Feature extraction of vibration signal of hydropower unit based on ceemdan sample entropy and pso-svm," *Engineering Journal of Wuhan University*, vol. 55, no. 1167-1175, 2022.
[19] F. Zhang, T.-Y. Wu, J.-S. Pan, G. Ding, and Z. Li, "Human motion recognition based on svm in vr art media interaction environment," *Human-centric Computing and Information Sciences*, vol. 9, no. 1, 2019. [Online]. Available: http://dx.doi.org/10.1186/s13673-019-0203-8
[20] X. Yao, "Application of optimized svm in sample classification," *International Journal of Advanced Computer Science and Applications*, vol. 13, no. 6, 2022.
[21] J. Mai, X. Wang, Z. Li, J. Liu, Z. Zhang, and H. Fu, "Eeg signal classification of tinnitus based on svm and sample entropy," *Computer Methods in Biomechanics and Biomedical Engineering*, vol. 26, no. 5, pp. 580–594, 2023.
[22] D. Bajić and N. Japundžić-Žigon, "On quantization errors in approximate and sample entropy," *Entropy*, vol. 24, no. 1, p. 73, 2022.
[23] H. Phan and A. Nguyen, "Deepface-emd: Re-ranking using patch-wise earth mover's distance improves out-of-distribution face identification," in *Proceedings of the IEEE/CVF Conference on Computer Vision and Pattern Recognition*, 2022, pp. 20 259–20 269.
[24] D. Meng, H. Wang, S. Yang, Z. Lv, Z. Hu, and Z. Wang, "Fault analysis of wind power rolling bearing based on emd feature extraction," *CMES-Computer Modeling in Engineering & Sciences*, vol. 130, no. 1, pp. 543–558, 2022.
[25] D. Chen, C. Cao, and B. Xhu, "Mallat research on applying mallat's pyramid algorithm to process one dimensional signal," *Journal of Chongqing University*, vol. 04, pp. 49–53, 1999.
[26] J. Pan, Z. Lu, and S. Sun, "Fast codeword search algorithm for image coding based on mean-variance pyramids of codewords," *Electronics Letters*, vol. 36, no. 3, p. 1, 2000.
[27] Q. Tang and Z. Gao, "Limitations of fourier transform and its improvement method," *Guangxi Physics*, vol. 2, pp. 17–20, 2003.
[28] Y. Zhang, X.-y. Lu, Q. Guo *et al.*, "Study of improved algorithm of image fusion of ct and mri based on pca and dtcwt," *China Medical Equipment*, vol. 19, no. 4, pp. 7–12, 2022.

[29] Y. Peng, "Fault diagnosis method of transformer winding based on wavelet transform," *Automation Application*, no. 10, pp. 141–142, 146, 2021.
[30] L. Li, J. Qian, and J.-S. Pan, "Characteristic region based watermark embedding with rst invariance and high capacity," *AEU-International Journal of Electronics and Communications*, vol. 65, no. 5, pp. 435–442, 2011.
[31] X. Guo and H. Cong, "Face recognition based on wavelet transform and multifeature fusion coding," *Laser & Optoelectronics Progress*, vol. 58, no. 12, pp. 301–311, 2021.
[32] Y. Du, C. He, and X. Wang, "Wavelet theory and vibration analysis," *Journal of Northeast Forestry University*, vol. 03, pp. 61–65, 1997.
[33] Z. Lyu, J. Luo, and X. Yang, "Application of hht time-frequency analysis technology in aeronautical test-rig bearing fault diagnosis based on wavelet packet and emd," *Measurement & Control Technology*, pp. 1–9.
[34] Y. Wang, L. Yu, C. Wang, F. Zuo, and Z. Wang, "Remote sensing image fusion algorithm based on improved his, pca and wavelet transform," *Computer & Digital Engineering*, vol. 49, no. 4, pp. 797–803, 2021.
[35] X. Guo, "Research on infrared lmage enhancement algorithm based on wavelet transform," *Microcontrollers & Embedded Systems*, vol. 21, no. 8, pp. 21–25, 2021.
[36] G. Zhou, P. Li, and L. Gao, "Research on denoising algorithm of pulse signal based on wavelet analysis transform," *Electronic Test*, pp. 50–52, 2021.
[37] J. Zhang, J. Shen, and J. Yuan, "Research on the electric energy metering data denoising algorithm of dc charging pile based on wavelet threshold denosing," *Electrical Measurement & Instrumentation*, pp. 1–9, 2022.
[38] J.-S. Pan and J.-W. Wang, "Texture segmentation using separable and non-separable wavelet frames," *IEICE Transactions on Fundamentals of Electronics, Communications and Computer Sciences*, vol. 82, no. 8, pp. 1463–1474, 1999.
[39] Y. Zhang, C. Ma, and P. Yang, "Face feature extraction algorithm based on wavelet transform and improved principal component analysis," *Journal of Jilin University(Science Edition)*, vol. 59, no. 6, pp. 1499–1503, 2021.
[40] J.-W. Wang, C.-H. Chen, and J.-S. Pan, "Genetic feature selection for texture classification using 2-d non-separable wavelet bases," *IEICE Transactions on Fundamentals of Electronics, Communications and Computer Sciences*, vol. 81, no. 8, pp. 1635–1644, 1998.
[41] Y. Zeng and G. Zhan, "Extracting cervical spine popping sound during neck movement and analyzing its frequency using wavelet transform," *Computers in Biology and Medicine*, vol. 141, p. 105126, 2022.